

**Figure 2** Behavior of  $\beta$  versus frequency.  $a_1 = 1$  mm,  $a_2 = 1.4$  mm,  $b = 2.3$  mm,  $c = 2.4$  mm,  $d = 3.12$  mm

IITA(Institute for Information Technology Advancement) [IITA-2006-(C1090-0603-0034)].

#### REFERENCES

1. J. Joubert and J.A.G. Malherbe, Moment method calculation of the propagation constant for leaky-wave modes in slotted rectangular waveguide, *IEE Proc Microwave Antenn Propag* 146 (1999), 411-415.
2. P. Lampariello, F. Frezza, H. Shigesawa, M. Tsuji, and A.A. Oliner, A versatile leaky-wave antenna based on stub-loaded rectangular waveguide: Part I-theory, *IEEE Trans Antenn Propag* 46 (1998), 1032-1055.
3. H.J. Eom and Y.H. Cho, Analysis of multiple groove guide, *Electron Lett* 35 (1999), 1749-1751.
4. M. Tsuji, H. Shigesawa, F. Frezza, P. Lampariello, and A.A. Oliner, A versatile leaky-wave antenna based on stub-loaded rectangular waveguide: Part III-comparisons with measurements, *IEEE Trans Antenn Propag* 46 (1998), 1047-1055.

© 2007 Wiley Periodicals, Inc.

## DIELECTRIC FILTER OPTIMAL DESIGN SUITABLE FOR MICROWAVE COMMUNICATIONS BY USING MULTI-OBJECTIVE EVOLUTIONARY ALGORITHMS

S. K. Goudos,<sup>1</sup> Z. D. Zaharis,<sup>1,2</sup> M. Salazar-Lechuga,<sup>3</sup> P. I. Lazaridis,<sup>2,4</sup> and P. B. Gallion<sup>4</sup>

<sup>1</sup> Telecommunications Centre, Aristotle University of Thessaloniki, 54124 Thessaloniki, Greece; Corresponding author: zaharis@auth.gr

<sup>2</sup> Department of Electronics, Alexander Technological Educational Institute of Thessaloniki, 57400 Thessaloniki, Greece

<sup>3</sup> School of Computer Science, University of Birmingham, Edgbaston, Birmingham, United Kingdom

<sup>4</sup> Département Communications et Electronique, Unité de Recherche Associée au Centre National de la Recherche Scientifique, 820 Ecole Nationale Supérieure des Télécommunications, 46 rue Barrault, 75634 Paris Cedex 13, France

Received 6 March 2007

**ABSTRACT:** A multiobjective evolutionary technique is applied to design dielectric filters useful in microwave communications technology.

The optimal geometry of the filters is derived by utilizing two different multiobjective optimization algorithms. The first one is the Nondominated Sorting Genetic Algorithm-II (NSGA-II), which is a popular multiobjective genetic algorithm. The second algorithm is based on multiobjective Particle Swarm Optimization with fitness sharing (MOPSO-fs). MOPSO-fs algorithm is a novel Pareto PSO algorithm that produces the Pareto front in a fast and efficient way. In the present work, MOPSO-fs is compared with NSGA-II to optimize the geometry of the filters under specific requirements concerning the frequency response of the filters. Several examples are studied to exhibit the efficiency of the multiobjective evolutionary optimizers and also the ability of the technique to derive optimal structures that can be used in practice. © 2007 Wiley Periodicals, Inc. *Microwave Opt Technol Lett* 49: 2324–2329, 2007; Published online in Wiley InterScience (www.interscience.wiley.com). DOI 10.1002/mop.22755

**Key words:** microwave filters; dielectric filters; multiobjective optimization; pareto optimization; particle swarm optimization; evolutionary programming; genetic algorithms

#### 1. INTRODUCTION

Microwave filter design is a common problem. Several design approaches exist in the literature [1–31]. Multilayer dielectric filter design under constraints has also been a favorite subject among researchers [32, 33]. Such design constraints require that the reflection coefficient value in the passband or stopband region should not lie, respectively above or below a predefined level. Evolutionary algorithms have been applied in multilayer dielectric filter design. In [32], a single objective approach is proposed. This is produced from the aggregation of the objective functions and a penalty term. Pareto optimization has been used in several practical electromagnetic design problems [34–36]. In [33], a multiobjective Genetic Algorithm (GA) is used for the generation of the Pareto front for the constraint dielectric filter design problem. The major drawback of a GA approach is the difficulty in the implementation due to the algorithm inherited complexity and the required long computational time.

Particle swarm optimization (PSO) [37] is an evolutionary computation method inspired by the social behavior of bird flocking. PSO algorithms are computationally efficient and can be easily implemented in practice. PSO has been used successfully in constrained or unconstrained electromagnetic design problems [38–54]. Multiobjective Particle Swarm Optimization with fitness sharing (MOPSO-fs) [55] is a novel Pareto PSO algorithm. MOPSO-fs is validated in [55] against highly competitive evolutionary multiobjective algorithms like Nondominated Sorting Genetic Algorithm-II (NSGA-II) [56]. In this article, both MOPSO-fs and NSGA-II are used for the constrained multilayer filter design problem. The Pareto fronts produced from these algorithms are compared and discussed. The advantages of the MOPSO-fs algorithm are shown.

#### 2. PROBLEM FORMULATION

The structure of the multilayer dielectric filter is shown in Figure 1. The unknown variables are the thickness and the electromagnetic characteristics of each layer. These characteristics are the frequency-dependent (in general) complex permittivity and permeability given by:

$$\varepsilon_i(f) = \varepsilon_0[\varepsilon'_i(f) - j\varepsilon''_i(f)] \quad (1)$$

$$\mu_i(f) = \mu_0[\mu'_i(f) - j\mu''_i(f)] \quad (2)$$

The terms  $\varepsilon_0$  and  $\mu_0$  are the free space permittivity and permeability, respectively. The filter is assumed to be composed of

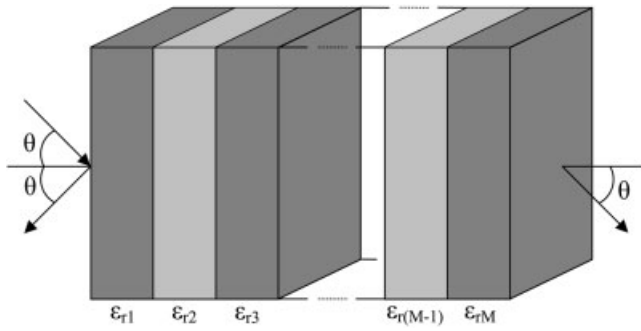


**Figure 1** Multilayer dielectric filter structure

lossless dielectric nonmagnetic materials ( $\epsilon_0 = 0$ ,  $\mu' = 1$ ,  $\mu'' = 0$ ), which have frequency independent real permittivity in the desired frequency range. Therefore, for a  $M$ -layer design problem, the number of the unknown variables is  $2M$ . For this type of multilayer structure, the general expression of the reflection coefficients  $R_i^{\text{TE}}$  and  $R_i^{\text{TM}}$  at the  $i$ th layer for the transverse electric (TE) and the transverse magnetic (TM) modes is respectively found by using the recursive formula [57]:

$$R_i^{\text{TE/TM}} = \frac{r_i^{\text{TE/TM}} + R_{i+1}^{\text{TE/TM}} e^{-2jk_i+1t_{i+1}}}{1 + r_i^{\text{TE/TM}} + R_{i+1}^{\text{TE/TM}} e^{-2jk_i+1t_{i+1}}} \quad i = M, M-1, \dots, 1 \quad (3)$$

$$R_{M+1}^{\text{TE/TM}} = r_{M+1}^{\text{TE/TM}} = \frac{n_M - n_0}{n_M + n_0} \quad (4)$$

$$r_i^{\text{TE/TM}} = \frac{n_{i-1} - n_i}{n_{i-1} + n_i} \quad i = 1, 2, \dots, M$$

$$n_i = \begin{cases} \sqrt{\epsilon'_i - \sin^2 \theta} & \text{TE mode} \\ \frac{\epsilon'_i}{\sqrt{\epsilon'_i - \sin^2 \theta}} & \text{TM mode} \end{cases} \quad (5)$$

$$k_i = \frac{2\pi f}{c \sqrt{\epsilon'_i}} \quad (6)$$

where  $M$  is the number of layers, and also  $t_i$  and  $\epsilon'_i$  are respectively the thickness and the dielectric constant of the  $i$ th layer. The microwave filter design problem is defined by the minimization of the objective functions given below:

$$f_1(x) = \sum_p [|R_{\text{TE}}(x, f_p)|^2 + |R_{\text{TM}}(x, f_p)|^2] \quad (7)$$

$$f_2(x) = \sum_s [(1 - |R_{\text{TE}}(x, f_s)|^2) + (1 - |R_{\text{TM}}(x, f_s)|^2)] \quad (8)$$

Moreover, the design problem is subject to the following constraints:

$$g_1(x) = 20 \log(R_{\text{TE}}(x, f_p)) < -10 \text{ dB} \quad (9)$$

$$g_2(x) = 20 \log(R_{\text{TM}}(x, f_p)) < -10 \text{ dB} \quad (10)$$

$$g_3(x) = 20 \log(R_{\text{TE}}(x, f_s)) > -5 \text{ dB} \quad (11)$$

$$g_4(x) = 20 \log(R_{\text{TM}}(x, f_s)) > -5 \text{ dB} \quad (12)$$

$$g_5(x) = T_{\text{tot}}(x) \leq T_{\text{des}} \quad (13)$$

where  $R_{\text{TE}}$  and  $R_{\text{TM}}$  are the reflection coefficients of the filter structure respectively for the transverse electric (TE) and the transverse magnetic (TM) modes,  $T_{\text{tot}}$  is the total layer thickness of the design found, and  $T_{\text{des}}$  is the desired total layer thickness. In addition,  $f_p$  and  $f_s$  define correspondingly the passband and the stopband frequency ranges, while  $f_p'$  and  $f_s'$  define respectively the passband and the stopband frequencies, where constraints must be satisfied. It is obvious that this type of multiobjective problem does not have a single global solution and it is often necessary to determine a set of points that all fit a predetermined definition for an optimum. Therefore, the main goal is to find a number of points that belong to the Pareto front. Then, optimal filter designs can be selected from this Pareto front. A multiobjective optimization evolutionary algorithm is used for this type of problem.

### 3. PARTICLE SWARM OPTIMIZATION

Particle swarm optimization (PSO) is a population-based stochastic optimization algorithm proposed by Eberhart and Kennedy in 1995 [37] and inspired by social behavior of birds. The particles move in the search space following the current best particles of the swarm. The swarm is initialized with a population of random particles (solutions) and searches for optima by updating the particle positions in every iteration. Each particle position is updated by following two optimum values. The first one is the best position achieved so far by the particle and is called *pbest*. The second one is the global best position obtained so far by any particle in the swarm. This best position is called *gbest*. After finding the *pbest* and *gbest*, the velocity of each particle is updated using a velocity update rule. Important parameters for PSO are the inertia weight  $w$ , and  $c_1$  and  $c_2$ , which are called learning factors. The inertia weight  $w$  can be a constant between 0.0 and 1.0 or can be linearly decreased from 0.9 to 0.4. This parameter represents the particle's fly without any external influence. The higher the value of  $w$ , the more the particle stays unaffected from *pbest* and *gbest*. The parameter  $c_1$  represents how much the particle is influenced from its best position, while the parameter  $c_2$  represents how much the particle is influenced from the swarm best position.

In a PSO algorithm, the parameters to be determined are the swarm size (or population size), which is usually 100 or less, the parameters  $c_1$  and  $c_2$  (usually both are set equal to 2.0 [37]), the inertia weight  $w$ , and the maximum number of iterations. PSO algorithm is inherently used only for real valued problems. An option to expand PSO for discrete valued problems also exists. A simple modification of the real-valued PSO, called binary PSO, has been presented by Kennedy and Eberhart [58].

#### 3.1. Multiobjective Particle Swarm Optimization with Fitness Sharing

Over the last years, researchers have proposed several multiobjective PSO algorithms. The MOPSO algorithm proposed in [59] has been successfully used [60] for the microwave absorber design problem. MOPSO-fs is a new and promising algorithm, which in [55] outperforms MOPSO. MOPSO-fs utilizes not only the PSO technique to guide the search, but also the fitness sharing to spread the solutions along the Pareto front. Fitness sharing [61] is used in the objective space and helps the algorithm to maintain diversity between solutions, so that particles within highly populated areas in the objective space are less likely to be followed. In each iteration of the algorithm, the best particles found (i.e., those

nondominated) are inserted into an external repository (or external memory). This repository helps to guide the search for the next generations and maintains a set of nondominated solutions until the end of the run. This set of solutions is what we are looking for, i.e., the set of solutions forming the Pareto front.

A brief description of the algorithm is as follows:

1. In the first step, all variables used by the algorithm are initialized. Particles ( $pop[i]$ ) are initialized inside the search space and their memories ( $pbest[i]$ ) are filled with the current positions. The external repository ( $gbest[i]$ ) is filled with all the nondominated particles. The fitness sharing ( $fShar[i]$ ) is calculated for each particle in the repository. According to the fitness sharing principle, particles (or solutions) that have more particles in their vicinity are less fit than those that have fewer particles surrounding their vicinity. The fitness sharing is given by:

$$fShar[i] = x/nCount_i \quad (14)$$

where  $x = 10$ . The value for  $x$  is arbitrarily chosen. A high value for  $fShar$  (close to or equal to 10) means that the particle is not surrounded by other particles or at least that there are particles not so close to this one. The denominator of the above expression is calculated by:

$$nCount_i = \sum_{j=0}^n sharing_i^j \quad (15)$$

where  $n$  is the number of particles in the repository and  $sharing_i^j$  is derived by:

$$sharing_i^j = \begin{cases} 1 - (d_i^j/\sigma_{share})^2 & \text{if } d < \sigma_{share} \\ 0 & \text{Otherwise} \end{cases} \quad (16)$$

$\sigma_{share}$  is the desired distance between any two particles, and  $d_i^j$  is the current Euclidean distance from the  $i$ th particle to the  $j$ th one.

2. Provided that a fitness sharing is assigned for each particle in the repository, some particles from the repository are chosen as leaders and they are going to be followed by all the other particles in the next iteration. The leaders will be chosen according to a stochastic universal sampling method (roulette wheel). Particles with higher levels of fitness are likely to be selected. This will allow them to explore places less explored in the search space. The velocity for the particles is updated according to the expression:

$$vel[i] = w \times vel[i] + c_1 \times r_1 \\ \times (pbest[i] - pop[i]) + c_2 \times r_2 \\ \times (gbest[h] - pop[i]) \quad (17)$$

where  $w$  is an inertia weight (a value of 0.4 was used in all cases),  $vel[i]$  is the velocity of the  $i$ th particle,  $r_1$  and  $r_2$  are random values between 0 and 1,  $c_1$  and  $c_2$  are random values between 1.49 and 2 (modification in their values was made for the dielectric filter design problem to increase the search space),  $pbest[i]$  is the best position found by the  $i$ th particle so far,  $gbest[h]$  is the particle to be followed, and  $pop[i]$  is the current position of the  $i$ th particle in the search space.

3. The new positions of the particles are calculated according to the velocities obtained in the previous step:

$$pop[i] = pop[i] + vel[i] \quad (18)$$

4. The repository is updated with the current solutions found by the particles. The criteria used to update the repository is the dominance and the fitness sharing. The particles that dominate the ones inside the repository will be inserted and all solutions dominated will be deleted. In this way, we maintain the repository as the Pareto front found so far. In the case where the repository is full of nondominated particles and a particle nondominated by any in the repository is found, their fitness sharing is compared. The fitness sharing is calculated for the new particle found. If it is better than the worst fitness sharing in the repository, then the particle with the worst fitness sharing is replaced by the new one. The fitness sharing for all the particles is updated when a particle is inserted in the repository or deleted from the repository. This is done to maintain fitness sharing in an up-to-date state in case the fitness sharing is used again when calculating velocities or when inserting particles into the repository.
5. Finally, the memory of each particle is updated according to the criterion of dominance. Therefore, if the current location of the particle dominates the previous one, the current location replaces the previous one in the particle's memory.

The results presented in the following section show that MOPSO-fs algorithm performs better in finding the Pareto front than NSGA-II (for the same population size).

#### 4. RESULTS

To compare the results with those given in [33], in all design cases the angle of incidence is set to  $\theta = 45^\circ$  and the filter is assumed to be composed of seven layers. The design frequency range is set from 24 GHz to 36 GHz. The same predefined material database as in [32, 33] was used. This database consists of 15 commercially available dielectric materials with real permittivity values of 1.01, 2.20, 2.33, 2.50, 2.94, 3.00, 3.02, 3.27, 3.38, 4.48, 4.50, 6.00, 6.15, 9.20, and 10.20. These values remain constant over the design frequency range. The thickness of each layer is varied between 1 and 10 mm.

MOPSO-fs and NSGA-II were applied for three design cases; a low-pass, a band-pass, and a band-stop filter. In all the results, the parameters chosen for MOPSO-fs were 100-particle swarm size, 100-particle repository size, 1000 iterations, and a sigma share value of 2. For NSGA-II, the population size was set equal to 100, 1000 generations were used, and finally the crossover and mutation probabilities were set respectively equal to 0.9 and 0.1 for both real and binary variables. Each algorithm runs for 10 times and the best results are compared.

The first example is a low-pass filter design case. The passband and stopband frequencies are set respectively to  $24 \text{ GHz} \leq f_p \leq 30 \text{ GHz}$  and  $30 \text{ GHz} \leq f_s \leq 36 \text{ GHz}$ . The range of constraints are set to  $24 \text{ GHz} \leq f_p < 28 \text{ GHz}$  and  $32 \text{ GHz} \leq f_s < 36 \text{ GHz}$ . The total desired thickness is set to 17 mm. A design example from the Pareto front is shown in Figure 2. This design has a total thickness of 16.24 mm compared with the thickness of 26.14 mm found in [33]. It is obvious that the new filter presents better behavior in the desired frequency range than the filter in [33]. The thicknesses of the layers are 6.725, 1.001, 1.007, 2.214, 1.376, 1.126, and 2.785 mm, and the corresponding dielectric constants are 2.33, 6, 2.33,

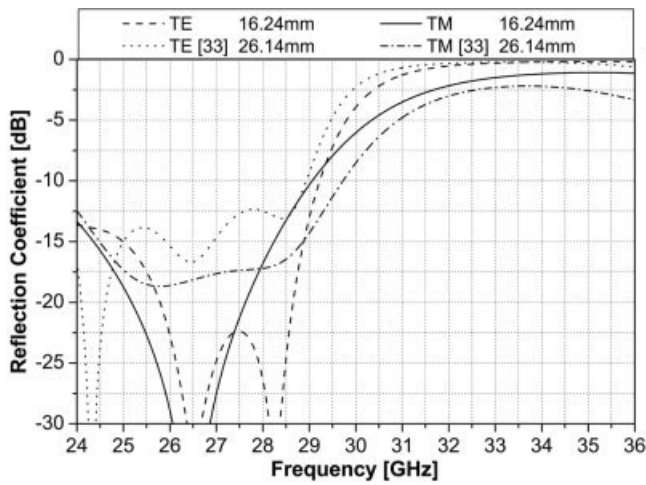


Figure 2 Frequency response of the low-pass filter

10.2, 2.2, 4.48, and 2.33. The Pareto front for this case is given in Figure 3. Each point of the Pareto front represents a feasible filter design case, which fulfils all the constraints. MOPSO-fs manages to find a larger dispersion of points in the front and clearly outperforms NSGA-II.

The next example concerns a constrained band-pass filter design. For this case, the passband and stopband frequencies are set to  $28 \text{ GHz} \leq f_p \leq 32 \text{ GHz}$  and  $24 \text{ GHz} \leq f_s \leq 28 \text{ GHz}$ ,  $32 \text{ GHz} \leq f_s \leq 36 \text{ GHz}$ . The range of constraints are set to  $29 \text{ GHz} \leq f_p < 31 \text{ GHz}$  and  $24 \text{ GHz} \leq f_s < 26 \text{ GHz}$ ,  $34 \text{ GHz} \leq f_s < 36 \text{ GHz}$ . The total desired thickness is set to 20 mm. Figure 4 presents a filter design case with 17.92 mm total thickness (instead of 33.44 mm found in [33]). For both TE and TM modes, the new design presents a similar or better behavior. The thicknesses of the layers are 4.719, 1.001, 4.921, 1.037, 1.018, 1.958, and 3.254 mm, while the corresponding dielectric constants are 2.2, 1.01, 10.2, 2.2, 4.5, 2.94, and 3.02. Figure 5 shows the Pareto front for the band-pass filter case. The position of the case of Figure 4 is shown in the Pareto front with an arrow. Again, MOPSO-fs produces better results compared with NSGA-II.

Finally, an example of a band-stop filter design is given. The lower and upper cutoffs are set respectively to 28 and 32 GHz. Thus, the passband and stopband frequencies are set to  $24 \text{ GHz} \leq f_p \leq 28 \text{ GHz}$ ,  $32 \text{ GHz} \leq f_p \leq 36 \text{ GHz}$ , and  $28 \text{ GHz} \leq f_s \leq 32 \text{ GHz}$ .

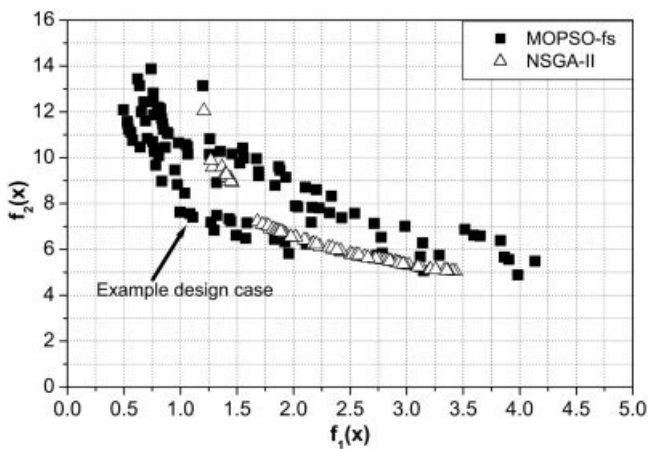


Figure 3 Pareto front found with MOPSO-fs and NSGA-II for the low-pass design

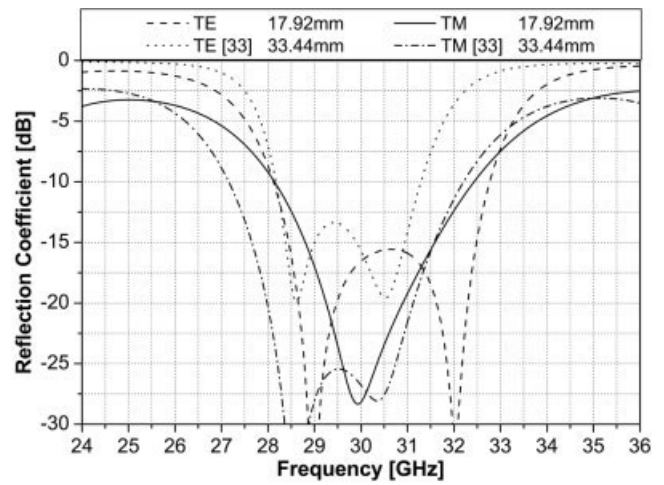


Figure 4 Frequency response of the band-pass filter

The range of constraints are set to  $24 \text{ GHz} \leq f_p < 26 \text{ GHz}$ ,  $34 \text{ GHz} \leq f_p < 36 \text{ GHz}$ , and  $29 \text{ GHz} \leq f_s < 31 \text{ GHz}$ . The total desired thickness is set to 21 mm. A band-stop filter design case is shown in Figure 6. The new filter found in this example is thinner than the band-stop filter found in [33] (20.53 mm instead of 29.25 mm). Moreover, this design has better frequency response for both TE and TM modes. The thicknesses of the layers are 1.605, 4.059, 4.723, 2.556, 1.228, 3.661, and 2.519 mm, and the dielectric constants are respectively 2.2, 9.2, 3.27, 9.2, 2.94, 6, and 3. The band-stop design case is more complex and difficult than the other cases. The number of points in the Pareto fronts found respectively by the two algorithms is about 60 instead of near 100 found in the other cases. The Pareto fronts found by both algorithms are shown in Figure 7. In this case, both algorithms perform in a similar manner. However, MOPSO-fs finds some points that are nondominated by others in the NSGA-II results. It must be noted that, in average, MOPSO-fs is faster by about 5–6 s than NSGA-II.

## 5. CONCLUSIONS

A novel microwave filter design method under constraints using MOPSO-fs has been presented. MOPSO-fs is a multiobjective PSO algorithm, which has been compared against NSGA-II. The above-presented sample cases are thinner and have a better frequency response than those found in the literature. Both algorithms

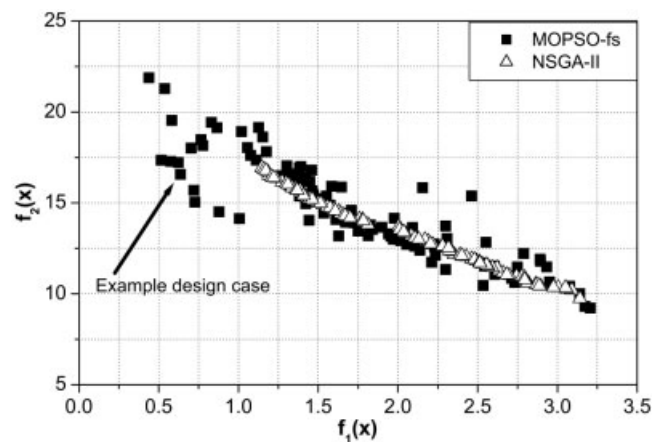


Figure 5 Pareto front found with MOPSO-fs and NSGA-II for the band-pass design

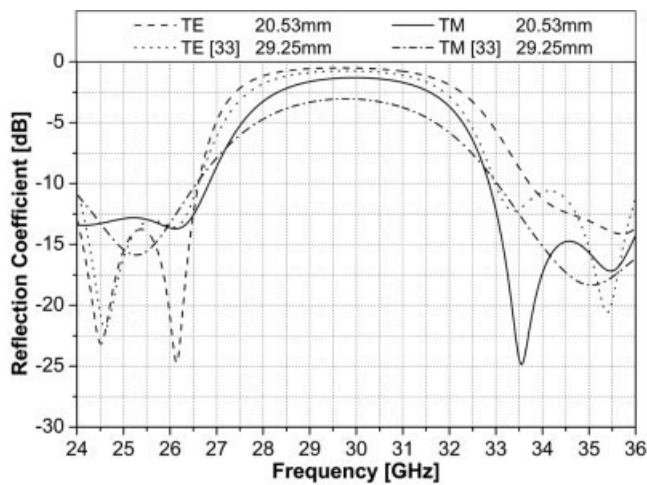


Figure 6 Frequency response of the band-stop filter

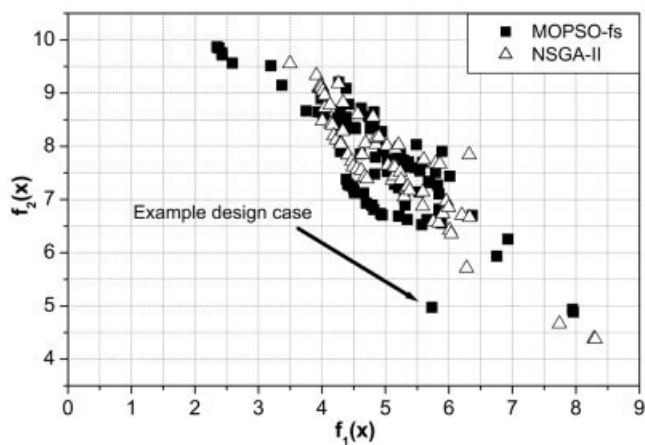


Figure 7 Pareto front found with MOPSO-fs and NSGA-II for the band-stop design

can be used to produce the Pareto front in all design cases. However, it is clear from the previous examples that MOPSO-fs can produce better results for the same population size and for the same number of generations. The main advantage of MOPSO-fs is the less computational load required than NSGA-II. This method can be used in conjunction with a numerical technique. In such a case, the computational time is an important issue. These practical design examples presented show the applicability and the efficiency of this method.

## REFERENCES

1. C.-C. Yu and K. Chang, Novel compact elliptic-function narrow-band bandpass filters using microstrip open-loop resonators with coupled and crossing lines, *IEEE Trans Microwave Theory Tech* 46 (1998), 952–958.
2. A. Toscano, F. Bilotti, and L. Vegni, A novel design method for tapered strip lines as microwave filters, *Microwave Opt Technol Lett* 24 (2000), 67–71.
3. S. Chakravarty and R. Mittra, Design of microwave filters using a binary-coded genetic algorithm, *Microwave Opt Technol Lett* 26 (2000), 162–166.
4. Y.-C. Chen and C.-L. Huang, A compact bandpass filter using dielectric resonators for cellular portable telephones, *Microwave Opt Technol Lett* 29 (2001), 359–362.

5. F. Liu and S. Xu, E-plane waveguide filters with partially filled dielectrics for wide bandwidth, *Microwave Opt Technol Lett* 31 (2001), 175–177.
6. L.-H. Hsieh and K. Chang, Slow-wave bandpass filters using ring or stepped-impedance hairpin resonators, *IEEE Trans Microwave Theory Tech* 50 (2002), 1795–1800.
7. M. G. Banciu, E. Ambikairajah, and R. Ramer, Microstrip filter design using FDTD and neural networks, *Microwave Opt Technol Lett* 34 (2002), 219–224.
8. M. Simeoni, S. Verdeyme, P. Guillon, and R. Sorrentino, Parasitic suppression in high-Q-factor dielectric loaded cavity filters, *Microwave Opt Technol Lett* 34 (2002), 344–347.
9. L.-H. Hsieh and K. Chang, Compact elliptic-function low-pass filters using microstrip stepped-impedance hairpin resonators, *IEEE Trans Microwave Theory Tech* 51 (2003), 193–199.
10. L.-H. Hsieh and K. Chang, Tunable microstrip bandpass filters with two transmission zeros, *IEEE Trans Microwave Theory Tech* 51 (2003), 520–525.
11. L.-H. Hsieh and K. Chang, Compact, low insertion-loss, sharp-rejection, and wide-band microstrip bandpass filters, *IEEE Trans Microwave Theory Tech* 51 (2003), 1241–1246.
12. N. Yang, Z.N. Chen, Y.Y. Wang, and M.Y.W. Chia, A two-layer compact electromagnetic bandgap (EBG) structure and its applications in microstrip filter design, *Microwave Opt Technol Lett* 37 (2003), 62–64.
13. O.-K. Lim, J.-I. Lee, Y.-J. Kim, and J.-Y. Park, A compact integrated band-pass filter on a low-dielectric constant polyimide dry film, *Microwave Opt Technol Lett* 40 (2004), 177–179.
14. C.-J. Wang, C.-H. Lin, and J.-W. Wu, A microstrip filter utilized in ultra-wideband antennas, *Microwave Opt Technol Lett* 41 (2004), 248–251.
15. W. Wang, Y. Lu, and J.S. Fu, Arbitrary planar microwave filter design by the EEM-GA approach, *Microwave Opt Technol Lett* 41 (2004), 276–279.
16. L.-S. Chen, M.-H. Weng, T.-H. Huang, H.-J. Chen, Y.-C. Hsi, and M.-P. Houng, A compact hairpin bandpass filter on high-permittivity dielectrics using a tape-casting technique, *Microwave Opt Technol Lett* 43 (2004), 164–166.
17. J. Wang, P. Liu, and Y. Li, TM<sub>010</sub> dielectric loaded cavity resonator for microwave filter, *Microwave Opt Technol Lett* 43 (2004), 373–376.
18. W.-H. Tu and K. Chang, Compact microstrip bandstop filter using open stub and spurline, *IEEE Microwave Wireless Compon Lett* 15 (2005), 268–270.
19. W.-H. Tu and K. Chang, Compact microstrip low-pass filter with sharp rejection, *IEEE Microwave Wireless Compon Lett* 15 (2005), 404–406.
20. S. Hong and K. Chang, Stub-tuned microstrip bandpass filters for millimeter-wave diplexer design, *IEEE Microwave Wireless Compon Lett* 15 (2005), 582–584.
21. T.-J. Baek, B.-S. Ko, D.-H. Shin, S.-C. Kim, B.-O. Lim, S.-K. Kim, H.-C. Park, and J.-K. Rhee, Fabrication of a band-reject filter using dielectric-supported air-gapped microstriplines, *Microwave Opt Technol Lett* 44 (2005), 1–4.
22. C.-L. Huang, C.-M. Tsai, A. Yang, and A. Hsu, Compact 5.8-GHz bandpass filter using stepped-impedance dielectric resonators for ISM band wireless communication, *Microwave Opt Technol Lett* 44 (2005), 421–423.
23. J.-S. Hong, H. Shaman, An optimum ultra-wideband microstrip filter, *Microwave Opt Technol Lett* 47 (2005), 230–233.
24. W.-H. Tu and K. Chang, Microstrip elliptic-function low-pass filters using distributed elements or slotted ground structure, *IEEE Trans Microwave Theory Tech* 54 (2006), 3786–3791.
25. C.-C. Chen, J.-T. Kuo, M. Jiang, and A. Chin, Study of parallel coupled-line microstrip filter in broadband, *Microwave Opt Technol Lett* 48 (2006), 373–375.
26. X. Guan, Z. Ma, P. Cai, T. Anada, and G. Hagiwara, A two-pole 900/1800-MHz microstrip filter for dual-band applications, *Microwave Opt Technol Lett* 48 (2006), 1388–1391.
27. Y.-W. Chen and M.-H. Ho, Design of microstrip filter and diplexer

- with a multiple harmonics suppression for mobile communication, *Microwave Opt Technol Lett* 48 (2006), 1812–1816.
28. S. Hong, H. Lee, H. Park, and J. Choi, A small bandstop microstrip filter for UWB applications, *Microwave Opt Technol Lett* 48 (2006), 2162–2165.
  29. E.A. Hashish and H.A. Saker, Full-wave analysis of a new designed wide band microstrip filter using the novel method of lines, *Microwave Opt Technol Lett* 49 (2007), 150–154.
  30. J.-F. Huang and Z.-M. Lyu, Design and implementation of a dualband microwave filter using nonuniform lines, *Microwave Opt Technol Lett* 49 (2007), 210–215.
  31. J. Yim, D. Kang, S. Son, and B. Kim, A planar-type dielectric resonator and filter using LTCC process, *Microwave Opt Technol Lett* 49 (2007), 578–581.
  32. A. Hoorfar, J. Zhu, and S. Nelatury, Electromagnetic optimization using a mixed-parameter self-adaptive evolutionary algorithm, *Microwave Opt Technol Lett* 39 (2003), 267–271.
  33. N.V. Venkatarayalu, T. Ray, and Y.-B. Gan, Multilayer dielectric filter design using a multiobjective evolutionary algorithm, *IEEE Trans Antennas Propagat* 53 (2005), 3625–3632.
  34. S.H. Yeung, W.T. Luk, H.K. Ng, K.F. Man, and C.H. Chan, A jumping genes paradigm for the design of wide-band patch antenna with double shorting wall, *Microwave Opt Technol Lett* 49 (2007), 706–709.
  35. D.S. Weile, E. Michielssen, and D.E. Goldberg, Genetic algorithm design of Pareto optimal broadband microwave absorbers, *IEEE Trans Electromagn Compat* 38 (1996), 518–525.
  36. S. Cui, A. Mohan, and D.S. Weile, Pareto optimal design of absorbers using a parallel elitist nondominated sorting genetic algorithm and the finite element-boundary integral method, *IEEE Trans Antennas Propagat* 53 (2005), 2099–2107.
  37. J. Kennedy and R.C. Eberhart, Particle swarm optimization, *IEEE Conf Neural Networks* 4 (1995), 1942–1948.
  38. J.R. Pérez and J. Basterrechea, Particle-swarm optimization and its application to antenna far-field-pattern prediction from planar scanning, *Microwave Opt Technol Lett* 44 (2005), 398–403.
  39. S. Mikki and A. Kishk, Improved particle swarm optimization technique using hard boundary conditions, *Microwave Opt Technol Lett* 46 (2005), 422–426.
  40. A.I.F. Vaz, A.I.P.N. Pereira, and E.M.G.P. Fernandes, Particle swarm and simulated annealing for multi-global optimization, *WSEAS Trans Inf Sci Appl* 2 (2005), 534–539.
  41. F. Azevedo and Z.A. Vale, Optimal short-term contract allocation using particle swarm optimization, *WSEAS Trans Inf Sci Appl* 2 (2005), 552–558.
  42. C. Jiang, Y. Ma, Y. Song, Y. Liu, J. Lu, and L. Wang, short-term power load forecasting using combination model with improved particle swarm optimization, *WSEAS Trans Inf Sci Appl* 2 (2005), 853–858.
  43. A. Kalos, Discrete particle swarm optimization for automating the design of multivariate autoregressive neural networks, *WSEAS Trans Inf Sci Appl* 2 (2005), 1807–1815.
  44. Y. Yang, R.S. Chen, and Z.B. Ye, Combination of particle-swarm optimization with least-squares support vector machine for FDTD time series forecasting, *Microwave Opt Technol Lett* 48 (2006), 141–144.
  45. A. Akdagli and K. Guney, New wide-aperture-dimension formula obtained by using a particle swarm optimization for optimum gain pyramidal horns, *Microwave Opt Technol Lett* 48 (2006), 1201–1205.
  46. S. Xu, Y. Rahmat-Samii, and D. Gies, Shaped-reflector antenna designs using particle swarm optimization: An example of a direct-broadcast satellite antenna, *Microwave Opt Technol Lett* 48 (2006), 1341–1347.
  47. R. Azaro, F. De Natale, M. Donelli, and A. Massa, Particle-swarm-optimizer-based optimization of matching loads for lossy transmission lines, *Microwave Opt Technol Lett* 48 (2006), 1485–1487.
  48. R. Azaro, M. Donelli, D. Franceschini, E. Zeni, and A. Massa, Optimized synthesis of a miniaturized SARSAT band pre-fractal antenna, *Microwave Opt Technol Lett* 48 (2006), 2205–2207.
  49. J. Horák, P. Chmela, L. Oliva, and Z. Raida, Multiband planar antennas on electromagnetic bandgap substrates: Complex global optimization of the structure, *Microwave Opt Technol Lett* 48 (2006), 2532–2534.
  50. B.S. Al-Kazemi, Velocity analysis for particle swarm optimization, *WSEAS Trans Inf Sci Appl* 3 (2006), 1807–1815.
  51. S.K. Goudos, A versatile software tool for microwave planar radar absorbing materials design using global optimization algorithms, *Master Des*, DOI: 10.1016/j.matdes. 2006.10.016.
  52. Z. Zaharis, D. Kampitaki, A. Papastergiou, A. Hatzigaidas, P. Lazaridis, and M. Spasos, Optimal design of a linear antenna array under the restriction of uniform excitation distribution using a particle swarm optimization based method, *WSEAS Trans Commun* 6 (2007), 52–59.
  53. Z.D. Zaharis, D.G. Kampitaki, P.I. Lazaridis, A.I. Papastergiou, A.T. Hatzigaidas, and P.B. Gallion, Improving the radiation characteristics of a base station antenna array using a particle swarm optimizer, *Microwave Opt Technol Lett*, accepted for publication.
  54. S.K. Goudos, Application of a particle swarm optimizer to the design of microwave broadband absorbers, *WSEAS Trans Commun* 6 (2007), 312–317.
  55. M. Salazar-Lechuga and J.E. Rowe, Particle swarm optimization and fitness sharing to solve multi-objective optimization problems, *Proc 2005 IEEE Congress Evol Comput* 2 (2005), 1204–1211.
  56. K. Deb, A. Pratap, S. Agarwal, and T. Meyarivan, A fast and elitist multiobjective genetic algorithm: NSGA-II, *IEEE Trans Evol Comput* 6 (2002), 182–197.
  57. W.C. Chew, *Waves and fields in inhomogeneous media*, IEEE Press, Piscataway, NJ, 1995.
  58. J. Kennedy and R.C. Eberhart, A discrete binary version of the particle swarm algorithm, *Proceedings of the 1997 IEEE Conference on Systems, Man, and Cybernetics*, IEEE Service Center, Piscataway, NJ, 1997, pp. 4104–4109.
  59. C.A. Coello Coello, G. Toscano Pulido, and M. Salazar Lechuga, Handling multiple objectives with particle swarm optimization, *IEEE Trans Evol Comput* 8 (2004), 256–279.
  60. S.K. Goudos and J.N. Sahalos, Microwave absorber optimal design using multi-objective particle swarm optimization, *Microwave Opt Technol Lett* 48 (2006), 1553–1558.
  61. D.E. Goldberg and J. Richardson, Genetic algorithms with sharing for multimodal function optimization, In: J.J. Grefenstette (Ed.), *Genetic algorithms and their application (Proceedings of the second international conference on genetic algorithms and their applications, Cambridge, MA, July 28–31, 1987)*, Erlbaum Associates, Hillsdale, MA, 1987, pp. 41–49.

© 2007 Wiley Periodicals, Inc.

## LOW-PHASE NOISE 3–42-GHz SIGNAL GENERATION USING HIGH-ORDER LONGITUDINAL MODES OF A COAXIAL LOOP CAVITY

Xinyue Wang and Ziyu Wang

Department of Electronics, State Key Laboratory on Advanced Optical Communication Systems and Networks, Peking University, Beijing 100871, People's Republic of China; Corresponding author: wangziyu@pku.edu.cn

Received 6 March 2007

**ABSTRACT:** This article demonstrates a novel coaxial loop cavity microwave/mm-wave generator. Working at high-order longitudinal modes, the generator has the single-sideband phase noise of about  $-75$  and  $-105$  dBc/Hz at 10 and 100 kHz offset over the frequency band of 3–42 GHz. © 2007 Wiley Periodicals, Inc. *Microwave Opt Technol Lett* 49: 2329–2331, 2007; Published online in Wiley InterScience (www.interscience.wiley.com). DOI 10.1002/mop.22754